HHS Public Access

Author manuscript

Oncogene. Author manuscript; available in PMC 2021 October 13.

Published in final edited form as:

Oncogene. 2021 May ; 40(18): 3331–3346. doi:10.1038/s41388-021-01764-y.

SCAMP3 is a mutant EGFR phosphorylation target and a tumor suppressor in lung adenocarcinoma

Abhilash Venugopalan[1,*], **Matthew Lynberg**[1], **Constance M. Cultraro**[1], **Khoa Dang P. Nguyen**[1], **Xu Zhang**[1], **Maryam Waris**[1], **Noelle Dayal**[1], **Asebot Abebe**[1], **Tapan K. Maity**[1], **Udayan Guha**[1,*,#]

[1]Thoracic and GI Malignancies Branch, Center for Cancer Research, NCI, NIH, Bethesda, MD.

Abstract

Mutations in the epidermal growth factor receptor (EGFR) tyrosine kinase domain constitutively activate EGFR resulting in lung tumorigenesis. Activated EGFR modulates downstream signaling by altering phosphorylation-driven interactions that promote growth and survival. Secretory Carrier Membrane Proteins (SCAMPs) are a family of transmembrane proteins that regulate recycling of receptor proteins, including EGFR. The potential role of SCAMPs in mutant EGFR function and tumorigenesis has not been elucidated. Using quantitative mass-spectrometry based phosphoproteomics, we identified SCAMP3 as a target of mutant EGFRs in lung adenocarcinoma and sought to further investigate the role of SCAMP3 in the regulation of lung tumorigenesis. Here we show that activated EGFR, either directly or indirectly phosphorylates SCAMP3 at Y86 and this phosphorylation increases the interaction of SCAMP3 with both wild type and mutant EGFRs. SCAMP3 knockdown increases lung adenocarcinoma cell survival and increases xenograft tumor growth *in vivo*, demonstrating a tumor suppressor role of SCAMP3 in lung tumorigenesis. The tumor suppressor function is a result of SCAMP3 promoting EGFR degradation and attenuating MAP kinase signaling pathways. SCAMP3 knockdown also increases multinucleated cells in culture, suggesting that SCAMP3 is required for efficient cytokinesis. The enhanced growth, increased colony formation, reduced EGFR degradation and multinucleation phenotype of SCAMP3 depleted cells were reversed by re-expression of wild type SCAMP3, but not SCAMP3 Y86F, suggesting that Y86 phosphorylation is critical for SCAMP3 function. Taken together, the results of this study demonstrate that SCAMP3 functions as a novel tumor suppressor in lung cancer by modulating EGFR signaling and cytokinesis that is partly Y86 phosphorylation dependent.

[*]**Corresponding author** Udayan Guha M.D., Ph.D., Thoracic and GI Malignancies Branch, Center for Cancer Research, National Cancer Institute, Building 10, Room 2B50C, Bethesda, MD 20892, udayan.guha@nih.gov; Abhilash Venugopalan Ph.D., Thoracic and GI Malignancies Branch, Center for Cancer Research, National Cancer Institute, Building 10, Room 3b52, Bethesda, MD 20892, abhilash.venugopalan@nih.gov.

Lead Contact: Udayan Guha, udayan.guha@nih.gov

[#]Current affiliation- Bristol Myers Squibb, Lawrenceville, NJ (employee) and Thoracic and GI Malignancies Branch, NCI, NIH (special volunteer).

Competing Interests Statement:

U.G. has a clinical trial agreement (CTA) with AstraZeneca and receives research funding from AstraZeneca, Esanex and Aurigene. The other authors have no conflicts of interest to report.

Introduction

Molecular profiling of lung cancer patients has led to the identification of driver mutations in multiple genes, including epidermal growth factor receptor (*EGFR*) [1, 2]. EGFR mutations, such as an in-frame deletion of the amino acids LREA within exon 19 ($EGFR^{Del}$) and an L858R substitution mutation ($EGFR^{L858R}$), constitutively activate EGFR thereby driving a cascade of proliferation and anti-apoptosis signals, which promote tumorigenesis [3-5]. Tumors harboring these EGFR gain of function mutations are sensitive to EGFR tyrosine kinase inhibitors (TKIs). Lung adenocarcinoma patients with $EGFR^{L858R}$ or $EGFR^{Del}$ mutations experience significant tumor shrinkage, prolonged progression-free survival (PFS) and overall survival (OS) when treated with erlotinib, a 1st generation EGFR-TKI, as opposed to standard chemotherapy [6]. Eventually, all patients with TKI sensitizing EGFR mutations will relapse after their initial response to TKIs. The most common mechanism of EGFR TKI acquired resistance to 1st and 2nd generation EGFR TKIs is the acquisition of a T790M mutation within the ATP-binding pocket of EGFR that accounts for 50-60% of acquired resistance [5, 7]. These driver mutations in the EGFR tyrosine kinase domain can alter its interaction dynamics by constitutive phosphorylation of its interaction partners as well as through the recruitment of new interaction partners that are hyperphosphorylation-dependent [8, 9]. Additionally, the sustained phosphorylation driven signaling can regulate spatial compartmentalization, which confers EGFR signaling specificity. Often these processes are driven by interactions that are mediated by phosphorylation. Therefore, it is essential to identify and characterize the targets of constitutively active mutant EGFRs that regulate EGFR receptor trafficking and signaling.

We, along with others, have performed global quantitative phosphoproteomic profiling of lung adenocarcinoma tumors and EGFR-driven lung adenocarcinoma cell lines thereby identifying several phosphotyrosine sites that are either hyperphosphorylated or hypo-phosphorylated [8, 10-13]. We have further characterized the role of phosphorylation at specific sites of proteins in regulating EGFR signaling and lung tumorigenesis and validated the phosphorylation changes at specific sites upon EGF stimulation or TKI inhibition by developing targeted assays [8, 14, 15]. Here, we utilized stable isotope labeling with amino acids in cell culture (SILAC) mass spectrometry and quantitative phosphoproteomics on the 11-18 lung adenocarcinoma cell line which harbors the $EGFR^{L858R}$ mutation and identified secretory carrier associated membrane protein 3 (SCAMP3) as a target of mutant EGFR. We selected SCAMP3 for further investigation because the potential role of SCAMP3 in EGFR-driven lung adenocarcinoma and the function of tyrosine phosphorylation of SCAMP3 Y86 has not been elucidated. SCAMP3 belongs to the SCAMP family, which are integral membrane proteins, localized to the plasma membrane, endosomes, extracellular vesicles, and trans-Golgi network [16-19]. SCAMP3 is known to regulate trafficking of receptors such as EGFR by generating multivesicular bodies (MVBs) in an EGF dependent manner, thereby regulating EGFR endosomal sorting and degradation [20]. SCAMP3 regulates EGFR trafficking by modulating ubiquitination, but its exact role in receptor recycling is not conclusive and may be context dependent [16-20]. SCAMP3 also directs amino acid transporters such as SLC1A5 to lysosomes [21]. Here, we demonstrate that SCAMP3 Y86 is phosphorylated downstream of EGFR signaling, including mutant EGFR signaling.

The interaction of SCAMP3 with either wild type or mutant EGFR is phosphorylation dependent. We further document a tumor suppressor role of SCAMP3 in human lung adenocarcinoma. Our findings demonstrate a heretofore unknown link between EGFR signaling and SCAMP3, which may contribute to tumor progression and resistance to EGFR targeted therapy.

Results:

Identification of EGFR regulated SCAMP3 phosphotyrosine sites by quantitative mass spectrometry

EGFR tyrosine kinase domain mutations such as L858R or LREA deletions constitutively activate EGFR, leading to autophosphorylation and phosphorylation of target proteins. This results in a constitutive signaling cascade, thereby promoting uncontrolled cell proliferation and tumorigenesis. We employed a mass spectrometry-based quantitative phosphoproteomics approach to identify proteins that are phosphorylation targets of mutant EGFRs [11]. We used SILAC to metabolically label 11-18 lung adenocarcinoma cells. Unlike most other EGFR mutant lung adenocarcinoma cells, the 11-18 cells that harbor the EGFR p.Leu858Arg (c.2573T>G) mutation do not overexpress mutant EGFR and these cells undergo growth arrest but not cell death upon EGFR TKI treatment [22, 23]. We investigated tyrosine phosphorylation in serum-starved (labeled with “light” Arg and Lys), EGF-stimulated (labeled with “medium” $^{13}C_6$-Arg and D_4-Lys), or EGF-stimulated cells with prior erlotinib treatment (labeled with “heavy” $^{13}C_6{}^{15}N_4$-Arg and $^{13}C_6{}^{15}N_2$-Lys) (Fig. 1A). Serum starved 11-18 cells had significant increase of EGFR phosphorylation in 3 minutes upon EGF stimulation that reduced significantly upon erlotinib treatment (Fig. 1B). Because erlotinib inhibits mutant EGFR, we expected a decrease in mutant EGFR-driven target phosphorylation upon drug treatment (“heavy” state of SILAC). Using this strategy, we identified hundreds of phosphorylation sites as potential EGFR targets. SCAMP3 was identified as one such phosphorylation target of mutant EGFR in lung adenocarcinoma cells. Representative mass-spectrometry spectrum of SCAMP3 Y86 containing peptide from 11-18 cells showed an increased mass-peak cluster with EGF stimulation (medium to light ratio=6.56), which decreased upon erlotinib treatment (heavy to medium ratio=0.17) (Fig. 1C & D). M/L ratio indicate the increased phosphorylation of SCAMP3 Y86 upon EGF stimulation compared to the serum starved state of 11-18 cells, and the H/M ratio indicates decreased Y86 phosphorylation upon erlotinib treatment prior to EGF stimulation. Together the tandem mass spectrometry data suggests SCAMP3 Y86 phosphorylation is a target of activated EGFR.

Sequence alignment across SCAMP orthologues indicate that Y86 is highly conserved in higher order species as shown by the sequence logo scale which quantitates the conservation (Fig. 1E & F), thereby suggesting the importance of Y86 in SCAMP3 function. SCAMP3 sequence alignments of its paralogues also show conservation of SCAMP3 Y86 between two SCAMP3 isoforms (Fig. 1G). In humans, the SCAMP family proteins (SCAMP1-3) possess cytoplasmic N-terminal sequences with NPF (Asn-Pro-Phe) repeats, four central transmembrane regions (TMRs), and a cytoplasmic tail [24]. SCAMP 4 and 5 are shorter and lack NPF repeats [24]. SCAMP3 has two isoforms encoded by two transcript variants.

These isoforms differ significantly because isoform 2 lacks exon 2 of SCAMP3; therefore, we investigated the expression pattern of both transcript variants in lung adenocarcinoma cells (Fig. 1H). We used this expression data to select two additional adenocarcinoma cell lines, A549, and H1975, which like 11-18, express significant levels of both SCAMP3 transcript variants, in roughly equal proportions. Taken together, these data suggest that SCAMP3 is a direct or indirect target of activated or mutant EGFR and is expressed in lung adenocarcinoma.

SCAMP3 phosphorylation is EGFR dependent and enhances SCAMP3-EGFR interaction

SCAMP3 is tyrosine phosphorylated and associates with EGFR upon EGF stimulation [15]. However, the interaction dynamics between SCAMP3 and mutant EGFR, which is constitutively phosphorylated in lung adenocarcinoma, is unknown. It is important to understand how these oncogenic EGFR mutations that drive lung adenocarcinoma alter the interaction of EGFR with SCAMP3. To gain mechanistic insight into the interaction of SCAMP3 with mutant EGFRs, we used HEK293T cells, which express undetectable levels of endogenous EGFR. We first generated HEK293T cells with stable expression of Flag-tagged SCAMP3. These cells were then transiently transfected with WT or mutant EGFR ($EGFR^{L858R}$, $EGFR^{Del}$, $EGFR^{L858R/T790M}$) (Fig. 2A). Transient expression of the wild type and mutant EGFRs was lower when SCAMP3 was stably expressed; the reduction was statistically significant among three biological replicates for WT and L858R EGFR while the reduction of Del EGFR and L858R/T790M EGFR had a trend without statistical significance (Fig. 2A, B). The decrease of transient EGFR expression was more pronounced for the mutant EGFRs. Immunoprecipitation experiments with FLAG-SCAMP3 showed that SCAMP3 was phosphorylated by both wild type and mutant EGFRs (Fig. 2C, D). We quantified the proportion of pSCAMP3 and total EGFR in SCAMP3 immunoprecipitates from three biological replicates that demonstrated that pSCAMP3 interaction with EGFR is significantly more in cells expressing the $EGFR^{L858R/T790M}$ compared to $EGFR^{WT}$, $EGFR^{L858R}$ and $EGFR^{Del}$ (Fig. 2C, D). Furthermore, both wild type and mutant EGFRs interacted with SCAMP3 and greater tyrosine phosphorylation of EGFR and SCAMP3 was associated with enhanced interaction (Fig. 2C). It is interesting to note that in the HEK293T system, constitutive phosphorylation of $EGFR^{Del}$ is lower as previously reported [5]. This decreased $EGFR^{Del}$ phosphorylation is accompanied by decreased SCAMP3 phosphorylation and reduced interaction with SCAMP3 (Fig. 2C). We identified Y86 and Y35 as phosphorylation sites on SCAMP3 in our mass spectrometry-based phosphoproteomic experiments [11]. Here, we sought to confirm whether Y35 and Y86 are the predominant phosphorylation sites of SCAMP3. We substituted tyrosine with phenylalanine to mimic unphosphorylated tyrosine thus allowing us to determine whether phosphorylation of SCAMP3 at Y35 or Y86 is important for the interaction with WT and mutant EGFRs. We transiently co-transfected HEK293T cells with WT EGFR or $EGFR^{L858R/T790M}$ together with SCAMP3 or SCAMP3 mutant (Y35F and Y86F) cDNA constructs (Fig. 2E). Cell extracts were immunoprecipitated with FLAG-specific antibodies (middle panel) and EGFR (lower panel) and immunoblotted as indicated (Fig. 2E). SCAMP3 phosphorylation was diminished in the Y35F and Y86F mutants, suggesting Y35 and Y86 are indeed the major SCAMP3 tyrosine phosphorylation sites (Fig. 2F). SCAMP3 immunoprecipitation demonstrated decreased interaction of SCAMP3 Y35F and Y86F

mutants with EGFR compared to WT SCAMP3 (Fig. 2G). Reciprocal immunoprecipitation was performed by immunoprecipitating EGFR that is expected to immunoprecipitate both endogenous and exogenous SCAMP3. EGFR immunoprecipitation indicated a significantly decreased interaction of exogenous SCAMP3-FLAG with EGFR-L858R/T790M in cells expressing SCAMP3 Y35F and Y86F mutants and with WT WEGFR in cells expressing SCAMP3 Y86F mutant (Fig. 2H). Taken together, we confirm that Y35 and Y86 are the major sites of tyrosine phosphorylation in SCAMP3 and Y86, as well as Y35 phosphorylation enhances the interaction of WT and L858R/T790M EGFR with SCAMP3.

Our quantitative phosphoproteomics screen of 11-18 cells demonstrated that the phosphorylation of SCAMP3 Y86 was decreased upon treatment with erlotinib, a first-generation EGFR tyrosine kinase inhibitor (TKI). Osimertinib is a third generation irreversible EGFR TKI that is now approved for the treatment of patients harboring the $EGFR^{T790M}$ resistant mutation as well as for front line treatment of all EGFR mutant patients [25]. We sought to further confirm whether interaction of EGFR and SCAMP3 is phosphorylation dependent and could be modulated by osimertinib treatment. We expressed $EGFR^{WT}$ or the mutant EGFRs in HEK293T cells stably expressing SCAMP3. Upon transient expression of the EGFRs for 72 hours, we treated the cells with either DMSO or osimertinib for 1 hour and then prepared cell lysates. As expected, EGFR phosphorylation significantly diminished upon osimertinib treatment and expression of EGFRs were comparable (input in Fig. 2I). Lysates were immunoprecipitated with FLAG antibody for SCAMP3 then immunoblotted with EGFR, SCAMP3 and pan-pTyr 4G10 antibodies. SCAMP3 showed increased phosphorylation in cells expressing the mutant EGFRs and the interaction mirrored the phosphorylation status of the WT and mutant EGFRs (Fig. 2I). SCAMP3 interaction with EGFRs ($EGFR^{WT}$, $EGFR^{Del}$ and $EGFR^{L858R/T790M}$) was significantly diminished upon treatment with EGFR-TKI, osimertinib (Fig. 2I, J), thereby further indicating that EGFR phosphorylation plays a critical role in the interaction of SCAMP3 with EGFR.

We sought to further validate these results by examining the regulation of endogenous EGFR and SCAMP3 in human lung adenocarcinoma cells. We used A549 which harbors $EGFR^{WT}$, and H1975, which harbors $EGFR^{L858R/T790M}$. These cells express both SCAMP3 isoforms (Fig. 1H). EGF stimulation of serum starved A549 cells increased phosphorylation of EGFR (Fig. 2K). Interaction of SCAMP3 and EGFR increased upon EGF stimulation but was inhibited upon osimertinib treatment, suggesting that increased phosphorylation of EGFR also increased interaction of SCAMP3 and EGFR (Fig. 2K). In H1975 cells harboring constitutively active $EGFR^{L858R/T790M}$, interaction of EGFR with SCAMP3 was similar in serum-starved state or upon EGF activation. However, upon osimertinib treatment, EGFR interaction with SCAMP3 was almost entirely abrogated (Fig. 2L). These findings delineate the differences in EGFR and SCAMP3 interaction in lung adenocarcinoma that harbor either $EGFR^{WT}$ or constitutively active mutant EGFR. Since A549 cells express $EGFR^{WT}$ that is unphosphorylated in basal serum starved state, an increased SCAMP3-EGFR interaction was observed upon EGF stimulation and $EGFR^{WT}$ phosphorylation, as predicted (Fig. 2K). However, in H1975 cells, there was no change in EGFR-SCAMP3 interaction upon EGF stimulation. This is likely due to saturation of SCAMP3 with interacting activated $EGFR^{L858R/T790M}$ in basal state; hence further increased phosphorylation of mutant EGFR

as evident in input did not result in increased interaction (Fig. 2L). To further validate if EGFR is the kinase upstream of SCAMP3 and whether the interaction of EGFR with SCAMP3 is dependent on phosphorylation of EGFR and SCAMP3, we transiently overexpressed kinase dead (K721A), WT and L858R/T790M EGFRs along with SCAMP3 in HEK293T cells (Fig. 2M). The tyrosine phosphorylation of SCAMP3 was abrogated in presence of kinase dead EGFR K721A and the interaction of EGFR K721A with SCAMP3 was significantly reduced compared to WT or EGFR- L858R/T790M (Fig. 2N, O). In summary, these data suggest that SCAMP3 phosphorylation requires EGFR kinase activity and increases its interaction with EGFR. Furthermore, Y86 and Y35 phosphorylation of SCAMP3 enhances the interaction of EGFR with SCAMP3. Although, phosphorylation of EGFR and SCAMP3 significantly increases their interaction, there is some residual interaction in the absence of phosphorylation (Fig 2N).

SCAMP3 depletion accelerates tumor growth in human lung adenocarcinoma cells expressing $EGFR^{WT}$

SCAMP3 is overexpressed in several cancer types [26-28]. Analysis of publicly available lung cancer data using cBioPortal suggested that SCAMP3 is overexpressed in patients with lung cancer (Fig. S1A)[29] . However, EGFR and SCAMP3 alterations in the TCGA data exhibit a tendency for mutual exclusivity (Fig. S1B). SCAMP3 is located within chromosome 1q22. Most genes within this region are co-amplified and overexpressed (Fig. S1C, D), suggesting that the selective pressure for 1q22 amplification and the resulting overexpression of genes in this location may not be due to SCAMP3 in particular.

Since the role of SCAMP3 in tumorigenesis is unknown, we investigated the consequences of depleting SCAMP3 in human lung adenocarcinoma cells using the CRISPR/Cas9 approach. We used two different cell lines, 1) A549 which expresses WT EGFR and a KRAS mutant, 2) H1975, which harbors EGFR L858R/T790M mutant. We selected A549 cells since mRNA expression analysis (Fig. 1H) showed that A549 expresses higher levels of SCAMP3. We selected H1975 cells which, in addition to a high SCAMP3 expression, also harbor the EGFR L858R/T790M mutation and we aimed to investigate the role of SCAMP3 in modulating response to osimertinib, a 3rd generation EGFR tyrosine kinase inhibitor.

We first depleted endogenous SCAMP3 in A549 cells and subsequently rescued with either WT SCAMP3 or SCAMP3 Y86F expression (Fig 3A). Upon SCAMP3 depletion, phosphorylation of ERK increased compared to control (ntsg) that was restored upon expression of WT SCAMP3, but not SCAMP3 Y86F (Fig 3B). It is to be noted that the rescue expression of either WT or SCAMP3-Y86F was lesser than the endogenous SCAMP3 expression. Moreover, intact Y35 phosphorylation in SCAMP3-Y86F mutant may provide residual function of SCAMP3. Hence the rescue with either the WT or Y86F mutant SCAMP3 may not be complete (Fig. 3A-B). Importantly, SCAMP3 depleted cells grew faster than the control cells and re-expression of WT SCAMP3, but not the SCAMP3 Y86F could rescue this phenotype (Fig 3C). Additionally, colony formation was significantly increased upon SCAMP3 depletion (Fig. 3D, E) and was rescued upon restoration of WT SCAMP3 but not by SCAMP3 Y86F mutant expression. The increased growth revealed by colony formation of A549 cells upon SCAMP3 depletion was evident in cells that

were depleted using three different sgRNAs (Fig. S2A-C). We also investigated whether the SCAMP3 depleted A549 cells had enhanced tumor growth in xenograft models *in vivo*. Consistent with the increased cell growth and colony formation seen in SCAMP3 depleted cells, tumor formation was accelerated in SCAMP3 depleted A549 xenografts. The increased growth phenotype could be rescued by re-expression of WT SCAMP3 (Fig. 3F). We confirmed that there was complete depletion of SCAMP3 protein upon CRISPR/Cas9-mediated *SCAMP3* knock-out and the re-expression of SCAMP3 protein in the rescue xenografts (Fig. 3G). Taken together, these data suggest that SCAMP3 negatively regulates tumor growth in lung adenocarcinoma cells that express wild type EGFR by regulating EGFR signaling.

SCAMP3 depletion accelerates tumor growth in human lung adenocarcinoma cells expressing $EGFR^{L858R/T790M}$ and may decrease sensitivity to EGFR TKI

We investigated the role of SCAMP3 in regulating growth of H1975 cells that harbor the $EGFR^{L858R/T790M}$ mutant. We hypothesized that SCAMP3 depletion will attenuate the growth inhibitory effects of osimertinib, a 3rd generation EGFR TKI that targets $EGFR^{L858R/T790M}$. We treated H1975 ntsgRNA (control) cells, and SCAMP3 depleted H1975 sg274 cells (Fig. 4A) either with DMSO (control) or osimertinib and assessed cell viability and colony formation. Viability and colony formation was enhanced in SCAMP3 depleted (sg274) as compared to control (ntsg) H1975 cells treated with either DMSO (Fig. 4B, C) or Osimertinib (Fig. 4D-E). We also confirmed increased growth of H1975 cells upon SCAMP3 knockdown with two different SCAMP3 sgRNAs (Fig. S3A-D). Osimertinib significantly inhibited cell growth of WT SCAMP3 expressing cells (ntsg) (Fig. 4C, F), as expected, while the effect was less pronounced upon loss of SCAMP3 expression (sg274) (Fig. 4E, F). We compared EGFR phosphorylation and downstream AKT and ERK signaling in SCAMP3 depleted cells to control by treating them with either DMSO or osimertinib for 1hour. Osimertinib treatment reduced EGFR, AKT, and ERK phosphorylation in SCAMP3 expressing cells, as expected, but not in SCAMP3 depleted cells (Fig. 4G). Moreover, this may also indicate that SCAMP3 may be involved in regulation of pathways other than EGFR, which helps in the increased growth even in the presence of EGFR-TKIs such as osimertinib. Additionally, SCAMP3 depleted H1975 cells also had enhanced xenograft tumor formation *in vivo* (Fig. 4H). We confirmed the lack of SCAMP3 expression in the xenograft tumors generated by SCAMP3 depleted cells (Fig. 4I). Additionally, SCAMP3 depleted tumors showed increased proliferation marker, Ki67 and ERK activation as assessed by pERK immunoreactivity (Fig. 4J, K and S3E).

Additionally, we used siRNAs to transiently knock down SCAMP3 in human lung adenocarcinoma cells (Fig. S4A). In these experiments in addition to A549 and H1975 cells, two other cell lines were used. We used 11-18 cells harboring $EGFR^{L858R}$, where we previously identified SCAMP3-Y86 phosphorylation by quantitative mass spectrometry, and PC9 cells that harbor the $EGFR^{Del746-750}$ mutant. Transient knockdown of SCAMP3 in these cells resulted in accelerated growth in cell culture (Fig. S4B-E). In summary, SCAMP3 targeting experiments described here show that SCAMP3 is a negative regulator of tumor growth and acts as a tumor suppressor in human lung adenocarcinoma *in vitro* and *in vivo*.

SCAMP3 enhances EGFR degradation upon EGF stimulation

SCAMP3 is a putative membrane trafficking protein that regulates endocytosis of RTKs such as EGFRs. Moreover, SCAMP3 regulates intraluminal vesicle formation in late endosomes, thereby sorting EGFR into multivesicular endosomes and promoting lysosome-targeted degradation [20]. In this study we have shown that SCAMP3 depletion increased MAP kinase signaling and accelerated tumor growth. We hypothesized that the observed phenotypes were partly mediated by the regulation of EGFR degradation by SCAMP3. Hence, we examined the effects of SCAMP3 depletion on EGFR degradation upon EGF stimulation. We used non-targeted sgRNA containing control, SCAMP3 depleted, and SCAMP3 depleted and subsequently rescued with either SCAMP3 WT or SCAMP3 Y86F mutant A549 cells for 3 biological replicates of EGFR degradation assays. These cells were serum starved, treated with cycloheximide to inhibit translation, then stimulated with EGF (100ng/ml). Upon EGF stimulation, the kinetics of EGFR degradation was delayed in SCAMP3 depleted A549 cells that could be rescued with WT SCAMP3 re-expression, but not SCAMP3 Y86F expression (Fig. 5A, B). EGFR was significantly degraded in control A549 cells within 30 minutes, but similar level of degradation was apparent only at 2 hours in SCAMP3 depleted cells. We also investigated the potential effects of SCAMP3 overexpression on EGFR degradation in 3 biological replicates of EGFR degradation assays in HEK293T cells modified to overexpress either SCAMP3 or SCAMP3 Y86F (Fig. 5C, D). Compared to control, cells overexpressing SCAMP3 exhibited accelerated EGFR degradation upon EGF stimulation. There was a statistically significant increased degradation upon SCAMP3 overexpression, but not with SCAMP3 Y86F expression. Taken together, our results suggest that SCAMP3 is a positive regulator of EGFR degradation and this function of SCAMP3 is Y86 phosphorylation dependent.

SCAMP3 depletion alters nuclear number and morphology in lung adenocarcinoma

Studies have shown that SCAMP family member proteins, SCAMP2 and SCAMP3, are necessary for cytokinesis, and depletion of SCAMP2 and 3 results in multinucleated cells [30]. Multinucleation has been associated with therapeutic resistance and tumor heterogeneity [31, 32]. Since SCAMP3 is necessary for secondary ingression and cytokinesis, we examined whether multinucleation is increased in A549 lung adenocarcinoma cells depleted of SCAMP3 expression and rescued by either WT SCAMP3 or SCAMP3 Y86F (Fig 6A). The nuclei of the cells were stained with Hoechst dye and the membrane/cytoplasm of the cells stained with β-catenin antibody (Fig. 6B). There was significant increase in cells having more than one nucleus upon SCAMP3 depletion, which was reversed by wild type SCAMP3, but not SCAMP3 Y86F expression (Fig. 6B, C). The morphology of the nuclei was also altered upon SCAMP3 depletion. Nuclei were smaller and also appeared fragmented in many cells. This suggests that SCAMP3 may regulate cytokinesis in lung adenocarcinoma cells and Y86 phosphorylation of SCAMP3 is essential for this process.

Discussion

The potential role of SCAMP3 in lung tumorigenesis has remained unexplored. In this study, we revealed several novel aspects of SCAMP3 function, including its tumor suppressor

role in lung cancer. We showed that SCAMP3 Y86 is a target of phosphorylation by activated WT EGFR or constitutively active mutant EGFR, such as EGFR L858R/T790M. This phosphorylation increases SCAMP3 interaction with activated EGFR that could be inhibited by EGFR TKIs (Fig. 6D, **left panel**). WT SCAMP3 promotes degradation of activated EGFR. SCAMP3 depletion reduces EGFR degradation, increases pERK/pAKT signaling, and increases multinucleation. The increased proliferation, decreased EGFR degradation, and multinucleation phenotype of SCAMP3 depleted cells could be rescued by WT SCAMP3, but not SCAMP3 Y86F mutant (Fig. 6D, **right panel**). Most importantly, we show that depletion of SCAMP3 in human lung adenocarcinoma cells increases growth both *in vitro* and *in vivo* that is rescued by re-expression of wild type SCAMP3, but not Y86F mutant, suggesting that SCAMP3 acts as a tumor suppressor in human lung adenocarcinoma. Taken together, we demonstrate a novel tumor suppressor role of SCAMP3 that is mediated, in part, by its regulation of EGFR turnover, MAP kinase signaling, and its role in cytokinesis, all of which are modulated by SCAMP3 Y86 phosphorylation (Fig. 6D).

WT EGFR signaling is tightly regulated by ligand induced activation followed by receptor endocytosis that is mediated by interaction with the endocytosis machinery [33]. Constitutive activation of mutant EGFRs deregulates EGFR trafficking [34]. The constitutive activation also results in impaired interaction with partners, such as CBL that mediate EGFR trafficking and degradation, thereby leading to increased signaling [8, 35, 36]. In our study, we found that SCAMP3 is phosphorylated more in EGFR L858R/T790M-expressing cells compared to WT EGFR-expressing cells (Fig. 2C, D, N and O). Moreover, Y86, as well as Y35 are major sites of SCAMP3 phosphorylation downstream of EGFRs which also regulate EGFR-SCAMP3 interaction, as evidenced by the decreased phosphorylation as well as interaction observed upon expressing SCAMP3 Y86F or Y35F instead of WT SCAMP3 (Fig. 2E-H). Activated EGFR either directly or indirectly by activating additional tyrosine kinases may regulate SCAMP3 phosphorylation. This is supported by almost complete abrogation of SCAMP3 tyrosine phosphorylation in the presence of kinase dead EGFR (Fig. 2N). Interestingly, significantly reduced, but residual EGFR-SCAMP3 interaction remains in the context of kinase dead EGFR. This could be a result of residual interaction in a complex that is not dependent on EGFR kinase activity.

To gain insight into the role SCAMP3 plays in regulating tumorigenesis promoted by the EGFR-MAPK pathway, we investigated its role in mediating the growth of human lung adenocarcinoma cells and tumors harboring WT or oncogenic mutant EGFR. Our results show that SCAMP3 acts as a tumor suppressor in both wild type and mutant EGFR-expressing lung adenocarcinoma. Depletion of SCAMP3 in lung adenocarcinoma cell lines results in increased proliferation, colony formation, and accelerated xenograft tumor growth (Fig. 3, 4). However, prior studies have shown that SCAMP3 is over expressed in several cancer types and its overexpression predicts poor prognosis [27, 28]. To better understand this apparent dichotomy, we analyzed publicly available TCGA cancer datasets using cBioPortal. Although this analysis showed SCAMP3 overexpression in lung cancer, further examination revealed that all genes mapping within SCAMP3 genomic location, 1q22, were coordinately overexpressed in cancer. In fact, genes mapping to chromosomal region, 1q22, are highly expressed in several cancer types [37]. We speculate that one

of the co-amplified and overexpressed genes, but not SCAMP3, is responsible for the selective advantage of amplification of 1q22 in cancer. One such co-amplified gene in 1q22 is *RAB25*. Overexpression of *RAB25* was associated with decreased progression free survival, overall survival and increased aggressiveness in ovarian and breast cancers [37, 38]. Moreover, particularly with respect to EGFR mutant lung adenocarcinoma, SCAMP3 and EGFR associated genetic alterations show a tendency of mutually exclusivity (Fig. S1B), suggesting that SCAMP3 genomic alterations may co-occur with WT EGFR rather than oncogenic mutant EGFRs in lung adenocarcinoma. Further studies are needed to examine possible protein expression or post-translational modification changes, such as tyrosine phosphorylation of Y86 and/or Y35 in SCAMP3 that may govern its tumor suppressor role in lung adenocarcinoma. The regulation of SCAMP3 transcript or protein expression is poorly understood. A recent study demonstrated that miRNA miR-27a/b-3p and transcription factor Peroxisome Proliferator Activated Receptor Gamma (PPARG) regulate SCAMP3 expression [39]. SCAMP3 expression may be modulated by altered expression of such transcription factors or miRNAs in cancer.

Exactly how SCAMP3 regulates EGFR sorting remains inconclusive, because one study shows that transient SCAMP3 knock down facilitates EGFR degradation whereas another shows it inhibits EGFR degradation [16, 20]. Here we show that SCAMP3 depletion stabilizes EGFR and overexpression of SCAMP3 in H3K293T cells accelerates EGFR degradation. Taken together, our EGFR degradation data suggest that SCAMP3 positively regulates EGFR degradation, and lack of SCAMP3 results in reduced degradation. As shown previously, this may be by facilitating the EGFR sorting into multivesicular bodies which we have not investigated in this manuscript [20]. Additionally, we demonstrated increased MAP kinase activation and cellular proliferation upon SCAMP3 depletion, which was rescued by expression of WT SCAMP3, but not by SCAMP3 Y86F mutant, suggesting SCAMP3 phosphorylation plays a significant role in regulating downstream EGFR signaling and for the tumor suppressor role of SCAMP3 in lung adenocarcinoma. Since SCAMP3 has been shown to control formation of EGF dependent intraluminal vesicle biogenesis thereby regulating EGFR sorting into multivesicular endosomes [20], we speculate that the depletion of SCAMP3 potentially increases membrane bound EGFR, which may be sufficient for continued signaling of MAP kinases and promoting proliferation. Prior studies have demonstrated that EGFR predominantly transduces signals at the plasma membrane and the fraction of EGFRs on plasma membrane is enough for the signaling of MAP kinase pathway [40, 41]. Since there is enhanced SCAMP3 phosphorylation and EGFR-SCAMP3 interaction within 3 minutes of EGF stimulation (Fig. 1,B, C, D and Fig. 2K), it is reasonable to postulate that the phosphorylation dependent SCAMP3-EGFR interaction is localized predominantly on the cell surface, which is upstream of EGF dependent multivesicular body generation and entry of EGFR to MVBs (Fig. 6D). This interaction between SCAMP3 and EGFR upon EGF stimulation enhances EGFR degradation and signal attenuation (Fig. 5A-D and Fig. 3A), potentially by sub-compartmentalizing the EGFR to endocytosis, eventually leading to degradation. Since we have observed SCAMP3-EGFR interaction early upon EGF stimulation and increased MAPK pathway activation upon SCAMP3 depletion, we propose that the depletion of SCAMP3 may increase cell surface localization of EGFR. As shown previously, this increased EGFR localization on plasma

membrane reduces endocytosis and increases downstream signaling leading to survival of cancer cells [34].

Previous research has shown that SCAMP3 and SCAMP2 are required for several steps of cytokinesis such as secondary ingression and abscission [30]. Our findings suggest additional regulation of SCAMP3-mediated cytokinesis; via SCAMP3 Y86 phosphorylation as evidenced by the rescue of the altered nuclear phenotype, including multiple and or/fragmented nuclei in individual cells, by the SCAMP3 Y86F mutant (Fig. 6B-C). The Y-F mutant SCAMP3 or absence of SCAMP3 may dysregulate cytokinesis-associated processes in which SCAMP3 plays a role, thereby altering cell division and tumor growth. Because multinucleated cells increase drug resistance [42, 43], SCAMP3 depletion also may contribute to osimertinib resistance by increasing multinucleated cells. This is further corroborated by the reduced effect of growth inhibition by osimertinib, the 3rd generation EGFR TKI on SCAMP3 depleted cells compared to the control cells (Fig. 4F). The potential role of downregulation of SCAMP3 expression in EGFR TKI resistance needs to be further explored in resistant tumors from EGFR mutated lung adenocarcinoma patients treated with EGFR TKIs.

In summary, our study demonstrates, for the first time, the interaction of SCAMP3 with EGFR and especially mutant EGFRs is enhanced by EGFR-dependent phosphorylation. EGFR, either directly or indirectly phosphorylates SCAMP3 Y86 and Y35, which regulates EGFR SCAMP3 interaction and SCAMP3 function. Most importantly, we found that SCAMP3 acts as a tumor suppressor in lung adenocarcinoma by regulating tumor proliferation through the regulation of EGFR sorting as well as AKT and ERK signaling.

Materials and Methods:

Cell culture, plasmids, lentiviral transduction and transient transfections

HEK293T, A549, H1975, and PC9 cells were obtained from ATCC. 11-18 cells were provided by Dr. Koichi Hagiwara. Details of cell culture, plasmids, lentiviral transduction and transient transfections are described in Supplementary Methods.

SILAC-based Quantitative Mass Spectrometry Experiment of 11-18 Cells

3-state SILAC labeling of 11-18 cells was performed using L-arginine and L-lysine (light), ^{13}C6-Arginine and D4-Lysine (medium), or ^{13}C6^{15}N4-Arginine and ^{13}C6^{15}N2-Lysine (heavy). The cells were then processed for mass spectrometry analysis as previously described [11]. Phosphopeptide enrichment was performed using PhosphoScan Kit (p-Tyr-100 and p-Tyr-1000, Cell Signaling, MA, USA) prior to mass spectrometry analyses. Details are provided in Supplementary Methods.

CRISPR/Cas9 gene editing and siRNA transfections

The lentiCRISPRv2, lentiCas9-Blast and lentiCRISPR-EGFPsgRNA (control) plasmids were gifts from Dr. Ji Luo at the NCI. To target SCAMP3 using the CRISPR/Cas9 approach, single-guide RNA (sgRNA) were designed using open source platforms (http://crispr.mit.edu) [44] and cloned into lentiCRISPRv2.

Context sequence for the three constructs used

sg271: AGAACTATGGCTCATACAGCACTCAGGTAC

sg272: TACCGGAAAGCCTTATACATGGGGCGGTAC

sg274: CGACTGGCGCAAGTCACCTGAAAGGGGTTG

Further details of siRNA transfections have been provided in Supplementary Methods.

Experimental mice

All animal experiments were reviewed and approved prior to animal use under the guidance of the IACUC of NCI/NIH. Mouse xenograft experiments were conducted in athymic nu/nu mice (6-12 weeks old). Details of mouse experiments are provided in Supplementary Methods.

Western blot and real-time PCR assays for expression analyses

Antibodies used for Western blot include Anti-EGFR (4267), anti-pEGFR (Y1068) (2234), anti-AKT, anti-pAKT(T308) (13038), anti-ERK (9102), anti-pERK1/2 (T202/T204) from Cell Signaling Technologies and anti-SCAMP3 antibody from Abcam. Details of Western blot and real-time PCR assays are provided in Supplementary Methods.

EGFR Degradation Assay

Cells were serum starved for 18 hours and treated with 100μM cycloheximide for 1 hour to inhibit protein synthesis. Cells were stimulated with EGF (100ng/ml) and cell lysates prepared at different times following EGF stimulation.

Microscopy and Hoechst 33342 staining

Cells were fixed and stained with β-Catenin and Hoechst 22242. Detailed methods are included in Supplementary Methods.

Histology and immunohistochemistry

Immunohistochemistry was performed as previously described[45]. Details are provided in Supplementary Methods.

Cell viability and colony formation assay

Cell proliferation was assessed by CellTitre-Glo assay according to manufacturer's protocol. Details of cell viability and colony formation assays are provided in Supplementary Methods.

Analysis of publicly available data sets

Lung adenocarcinoma data from TCGA PanCancer Atlas was analyzed using cbioportal (https://www.cbioportal.org/) with its default settings. Briefly, the parameters include mutation and mRNA expression Z scores (threshold ± 2.0).

Statistical analyses

All data represented herein were performed in 3 or more replicates and are presented as the mean ± SEM, unless otherwise indicated. Differences among groups were analyzed using t-test. Multiple testing was also performed for data in figures 2G, 3C and 3E using two-stage step-up Benjamini, Krieger and Yekutieli method. When overall analysis revealed significance among groups, means were compared and tested using Tukey *post hoc* analysis. Statistical significance was set at $P < 0.05$. All statistical analyses were performed in Prism 7 software (GraphPad Software).

Supplementary Material

Refer to Web version on PubMed Central for supplementary material.

Acknowledgements:

We thank Gaga Geneti for the assistance with the mice handling and treatments. This research was supported by the NIH Intramural Research Program, Center of Cancer Research, National Cancer Institute.

References:

1. Brose MS, Volpe P, Feldman M, Kumar M, Rishi I, Gerrero R et al. BRAF and RAS mutations in human lung cancer and melanoma. Cancer Res 2002; 62: 6997–7000. [PubMed: 12460918]
2. Gazdar AF. Activating and resistance mutations of EGFR in non-small-cell lung cancer: role in clinical response to EGFR tyrosine kinase inhibitors. Oncogene 2009; 28 Suppl 1: S24–31. [PubMed: 19680293]
3. Lynch TJ, Bell DW, Sordella R, Gurubhagavatula S, Okimoto RA, Brannigan BW et al. Activating mutations in the epidermal growth factor receptor underlying responsiveness of non-small-cell lung cancer to gefitinib. N Engl J Med 2004; 350: 2129–2139. [PubMed: 15118073]
4. Paez JG, Janne PA, Lee JC, Tracy S, Greulich H, Gabriel S et al. EGFR mutations in lung cancer: correlation with clinical response to gefitinib therapy. Science 2004; 304: 1497–1500. [PubMed: 15118125]
5. Pao W, Miller VA, Politi KA, Riely GJ, Somwar R, Zakowski MF et al. Acquired resistance of lung adenocarcinomas to gefitinib or erlotinib is associated with a second mutation in the EGFR kinase domain. PLoS Med 2005; 2: e73. [PubMed: 15737014]
6. Rosell R, Carcereny E, Gervais R, Vergnenegre A, Massuti B, Felip E et al. Erlotinib versus standard chemotherapy as first-line treatment for European patients with advanced EGFR mutation-positive non-small-cell lung cancer (EURTAC): a multicentre, open-label, randomised phase 3 trial. Lancet Oncol 2012; 13: 239–246. [PubMed: 22285168]
7. Stewart EL, Tan SZ, Liu G, Tsao MS. Known and putative mechanisms of resistance to EGFR targeted therapies in NSCLC patients with EGFR mutations-a review. Transl Lung Cancer Res 2015; 4: 67–81. [PubMed: 25806347]
8. Maity TK, Venugopalan A, Linnoila I, Cultraro CM, Giannakou A, Nemati R et al. Loss of MIG6 Accelerates Initiation and Progression of Mutant Epidermal Growth Factor Receptor-Driven Lung Adenocarcinoma. Cancer Discov 2015; 5: 534–549. [PubMed: 25735773]
9. Wei Y, Zou Z, Becker N, Anderson M, Sumpter R, Xiao G et al. EGFR-mediated Beclin 1 phosphorylation in autophagy suppression, tumor progression, and tumor chemoresistance. Cell 2013; 154: 1269–1284. [PubMed: 24034250]
10. Zhang X, Belkina N, Jacob HK, Maity T, Biswas R, Venugopalan A et al. Identifying novel targets of oncogenic EGF receptor signaling in lung cancer through global phosphoproteomics. Proteomics 2015; 15: 340–355. [PubMed: 25404012]
11. Zhang X, Maity T, Kashyap MK, Bansal M, Venugopalan A, Singh S et al. Quantitative Tyrosine Phosphoproteomics of Epidermal Growth Factor Receptor (EGFR) Tyrosine Kinase Inhibitor-

treated Lung Adenocarcinoma Cells Reveals Potential Novel Biomarkers of Therapeutic Response. Mol Cell Proteomics 2017; 16: 891–910. [PubMed: 28331001]

12. Zhang X, Maity TK, Ross KE, Qi Y, Cultraro CM, Gao S et al. Global proteome and phosphoproteome alterations in third generation EGFR TKI resistance reveal drug targets to circumvent resistance. bioRxiv 2020: 2020.2007.2004.187617.
13. Rikova K, Guo A, Zeng Q, Possemato A, Yu J, Haack H et al. Global survey of phosphotyrosine signaling identifies oncogenic kinases in lung cancer. Cell 2007; 131: 1190–1203. [PubMed: 18083107]
14. Awasthi S, Maity T, Oyler BL, Zhang X, Goodlett DR, Guha U. Dataset describing the development, optimization and application of SRM/MRM based targeted proteomics strategy for quantification of potential biomarkers of EGFR TKI sensitivity. Data Brief 2018; 19: 424–436. [PubMed: 29900338]
15. Awasthi S, Maity T, Oyler BL, Qi Y, Zhang X, Goodlett DR et al. Quantitative targeted proteomic analysis of potential markers of tyrosine kinase inhibitor (TKI) sensitivity in EGFR mutated lung adenocarcinoma. J Proteomics 2018; 189: 48–59. [PubMed: 29660496]
16. Aoh QL, Castle AM, Hubbard CH, Katsumata O, Castle JD. SCAMP3 negatively regulates epidermal growth factor receptor degradation and promotes receptor recycling. Mol Biol Cell 2009; 20: 1816–1832. [PubMed: 19158374]
17. Castle A, Castle D. Ubiquitously expressed secretory carrier membrane proteins (SCAMPs) 1-4 mark different pathways and exhibit limited constitutive trafficking to and from the cell surface. J Cell Sci 2005; 118: 3769–3780. [PubMed: 16105885]
18. Thomas P, Wohlford D, Aoh QL. SCAMP 3 is a novel regulator of endosomal morphology and composition. Biochem Biophys Res Commun 2016; 478: 1028–1034. [PubMed: 27507217]
19. Wu TT, Castle JD. Tyrosine phosphorylation of selected secretory carrier membrane proteins, SCAMP1 and SCAMP3, and association with the EGF receptor. Mol Biol Cell 1998; 9: 1661–1674. [PubMed: 9658162]
20. Falguieres T, Castle D, Gruenberg J. Regulation of the MVB pathway by SCAMP3. Traffic 2012; 13: 131–142. [PubMed: 21951651]
21. Beaumatin F, O'Prey J, Barthet VJA, Zunino B, Parvy JP, Bachmann AM et al. mTORC1 Activation Requires DRAM-1 by Facilitating Lysosomal Amino Acid Efflux. Mol Cell 2019; 76: 163–176 e168. [PubMed: 31492633]
22. Tabara K, Kanda R, Sonoda K, Kubo T, Murakami Y, Kawahara A et al. Loss of activating EGFR mutant gene contributes to acquired resistance to EGFR tyrosine kinase inhibitors in lung cancer cells. PLoS One 2012; 7: e41017. [PubMed: 22815900]
23. Gao SP, Mark KG, Leslie K, Pao W, Motoi N, Gerald WL et al. Mutations in the EGFR kinase domain mediate STAT3 activation via IL-6 production in human lung adenocarcinomas. J Clin Invest 2007; 117: 3846–3856. [PubMed: 18060032]
24. Singleton DR, Wu TT, Castle JD. Three mammalian SCAMPs (secretory carrier membrane proteins) are highly related products of distinct genes having similar subcellular distributions. J Cell Sci 1997; 110 (Pt 17): 2099–2107. [PubMed: 9378760]
25. Soria JC, Ohe Y, Vansteenkiste J, Reungwetwattana T, Chewaskulyong B, Lee KH et al. Osimertinib in Untreated EGFR-Mutated Advanced Non-Small-Cell Lung Cancer. N Engl J Med 2018; 378: 113–125. [PubMed: 29151359]
26. Ghosh D, Ulasov IV, Chen L, Harkins LE, Wallenborg K, Hothi P et al. TGFbeta-Responsive HMOX1 Expression Is Associated with Stemness and Invasion in Glioblastoma Multiforme. Stem Cells 2016; 34: 2276–2289. [PubMed: 27354342]
27. Suarez-Arroyo IJ, Feliz-Mosquea YR, Perez-Laspiur J, Arju R, Giashuddin S, Maldonado-Martinez G et al. The proteome signature of the inflammatory breast cancer plasma membrane identifies novel molecular markers of disease. Am J Cancer Res 2016; 6: 1720–1740. [PubMed: 27648361]
28. Zhang X, Sheng J, Zhang Y, Tian Y, Zhu J, Luo N et al. Overexpression of SCAMP3 is an indicator of poor prognosis in hepatocellular carcinoma. Oncotarget 2017; 8: 109247–109257. [PubMed: 29312605]

29. Gao J, Aksoy BA, Dogrusoz U, Dresdner G, Gross B, Sumer SO et al. Integrative analysis of complex cancer genomics and clinical profiles using the cBioPortal. Sci Signal 2013; 6: pl1. [PubMed: 23550210]
30. Schiel JA, Simon GC, Zaharris C, Weisz J, Castle D, Wu CC et al. FIP3-endosome-dependent formation of the secondary ingression mediates ESCRT-III recruitment during cytokinesis. Nat Cell Biol 2012; 14: 1068–1078. [PubMed: 23000966]
31. Diaz-Carballo D, Saka S, Klein J, Rennkamp T, Acikelli AH, Malak S et al. A Distinct Oncogenerative Multinucleated Cancer Cell Serves as a Source of Stemness and Tumor Heterogeneity. Cancer Res 2018; 78: 2318–2331. [PubMed: 29440172]
32. Mirzayans R, Andrais B, Murray D. Roles of Polyploid/Multinucleated Giant Cancer Cells in Metastasis and Disease Relapse Following Anticancer Treatment. Cancers (Basel) 2018; 10.
33. Avraham R, Yarden Y. Feedback regulation of EGFR signalling: decision making by early and delayed loops. Nat Rev Mol Cell Biol 2011; 12: 104–117. [PubMed: 21252999]
34. Tomas A, Futter CE, Eden ER. EGF receptor trafficking: consequences for signaling and cancer. Trends Cell Biol 2014; 24: 26–34. [PubMed: 24295852]
35. Walsh AM, Lazzara MJ. Differential parsing of EGFR endocytic flux among parallel internalization pathways in lung cancer cells with EGFR-activating mutations. Integr Biol (Camb) 2014; 6: 312–323. [PubMed: 24445374]
36. Padron D, Sato M, Shay JW, Gazdar AF, Minna JD, Roth MG. Epidermal growth factor receptors with tyrosine kinase domain mutations exhibit reduced Cbl association, poor ubiquitylation, and down-regulation but are efficiently internalized. Cancer Res 2007; 67: 7695–7702. [PubMed: 17699773]
37. Cheng KW, Lahad JP, Kuo WL, Lapuk A, Yamada K, Auersperg N et al. The RAB25 small GTPase determines aggressiveness of ovarian and breast cancers. Nat Med 2004; 10: 1251–1256. [PubMed: 15502842]
38. Glubb DM, Johnatty SE, Quinn MCJ, O'Mara TA, Tyrer JP, Gao B et al. Analyses of germline variants associated with ovarian cancer survival identify functional candidates at the 1q22 and 19p12 outcome loci. Oncotarget 2017; 8: 64670–64684. [PubMed: 29029385]
39. Kulyte A, Kwok KHM, de Hoon M, Carninci P, Hayashizaki Y, Arner P et al. MicroRNA-27a/b-3p and PPARG regulate SCAMP3 through a feed-forward loop during adipogenesis. Sci Rep 2019; 9: 13891. [PubMed: 31554889]
40. Pinilla-Macua I, Grassart A, Duvvuri U, Watkins SC, Sorkin A. EGF receptor signaling, phosphorylation, ubiquitylation and endocytosis in tumors in vivo. Elife 2017; 6.
41. Pinilla-Macua I, Watkins SC, Sorkin A. Endocytosis separates EGF receptors from endogenous fluorescently labeled HRas and diminishes receptor signaling to MAP kinases in endosomes. Proc Natl Acad Sci U S A 2016; 113: 2122–2127. [PubMed: 26858456]
42. Mittal K, Donthamsetty S, Kaur R, Yang C, Gupta MV, Reid MD et al. Multinucleated polyploidy drives resistance to Docetaxel chemotherapy in prostate cancer. Br J Cancer 2017; 116: 1186–1194. [PubMed: 28334734]
43. Parekh A, Das S, Parida S, Das CK, Dutta D, Mallick SK et al. Multi-nucleated cells use ROS to induce breast cancer chemo-resistance in vitro and in vivo. Oncogene 2018; 37: 4546–4561. [PubMed: 29743594]
44. Ran FA, Hsu PD, Wright J, Agarwala V, Scott DA, Zhang F. Genome engineering using the CRISPR-Cas9 system. Nat Protoc 2013; 8: 2281–2308. [PubMed: 24157548]
45. Venugopalan A, Lee MJ, Niu G, Medina-Echeverz J, Tomita Y, Lizak MJ et al. EGFR-targeted therapy results in dramatic early lung tumor regression accompanied by imaging response and immune infiltration in EGFR mutant transgenic mouse models. Oncotarget 2016; 7: 54137–54156. [PubMed: 27494838]

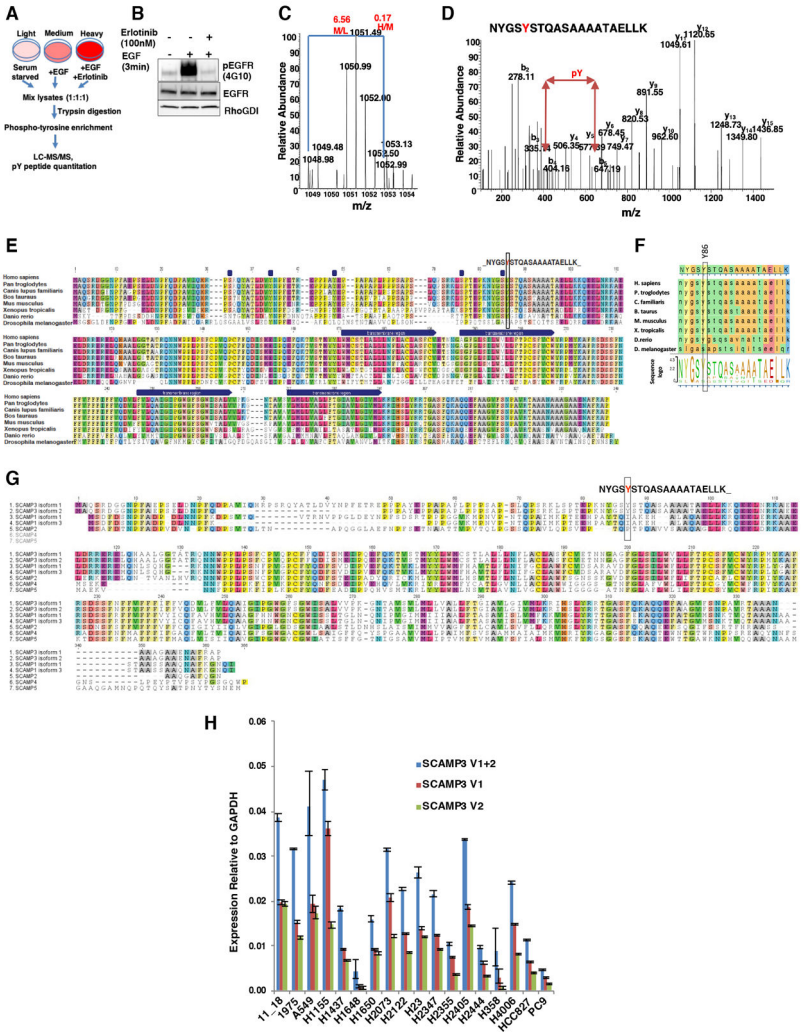

Figure 1. Identification of EGFR regulated SCAMP3 phosphotyrosine sites by quantitative mass spectrometry

A, Experimental design for SILAC-based quantitative phosphoproteomics by mass spectrometry. **B**, 11-18 cells were serum starved and either stimulated with EGF (100ng/ml) for 3 minutes or treated with erlotinib for 1 hour and then stimulated with EGF. Cells were lysed and immunoblotted with EGFR, pEGFR (4G10) and loading control, RhoGDI. **C**, Representative MS spectrum of a Y86-containing SCAMP3 peptide from TKI sensitive, 11-18 lung adenocarcinoma cells indicates that Y86 phosphorylation is increased in the presence of EGF (M/L), however, it is significantly inhibited by erlotinib (TKI) treatment (H/M). Relative abundances of individual labeled peptides under different treatment conditions were quantified by SILAC ratios and are shown at the top of the spectrum [EGF/serum starved: medium (M)/light (L), and EGF + erlotinib heavy (H)/M]. **D**, Representative MS and MS-MS spectra of the SCAMP3 Y86–containing peptide identified from *EGFR*^{L858R} driven 11-18 cells reveals phosphorylation of SCAMP3 at Y86. **E**, Multiple alignment of SCAMP3 orthologues shows the conserved regions including the Y86 residue. The peptide we identified by quantitative proteomics was also shown. **F,** Multiple alignment of phosphorylated SCAMP3 peptide that we identified shows Y86 is

significantly conserved among SCAMP3 orthologues as noted by sequence logo scale. **G,** Multiple alignment of SCAMP paralogues, including SCAMP1 and 2 isoforms with the conserved Y86 residue highlighted. The Y86 peptide, we identified by quantitative proteomics is shown. **H,** Expression of SCAMP3 V1 (isoform 1) and V2 (isoform 2) in a panel of human lung adenocarcinoma cell lines was determined by quantitative RT-PCR with *GAPDH* mRNA as an endogenous control. Samples were analyzed in quadruplicate, and values expressed as the mean ± SD.

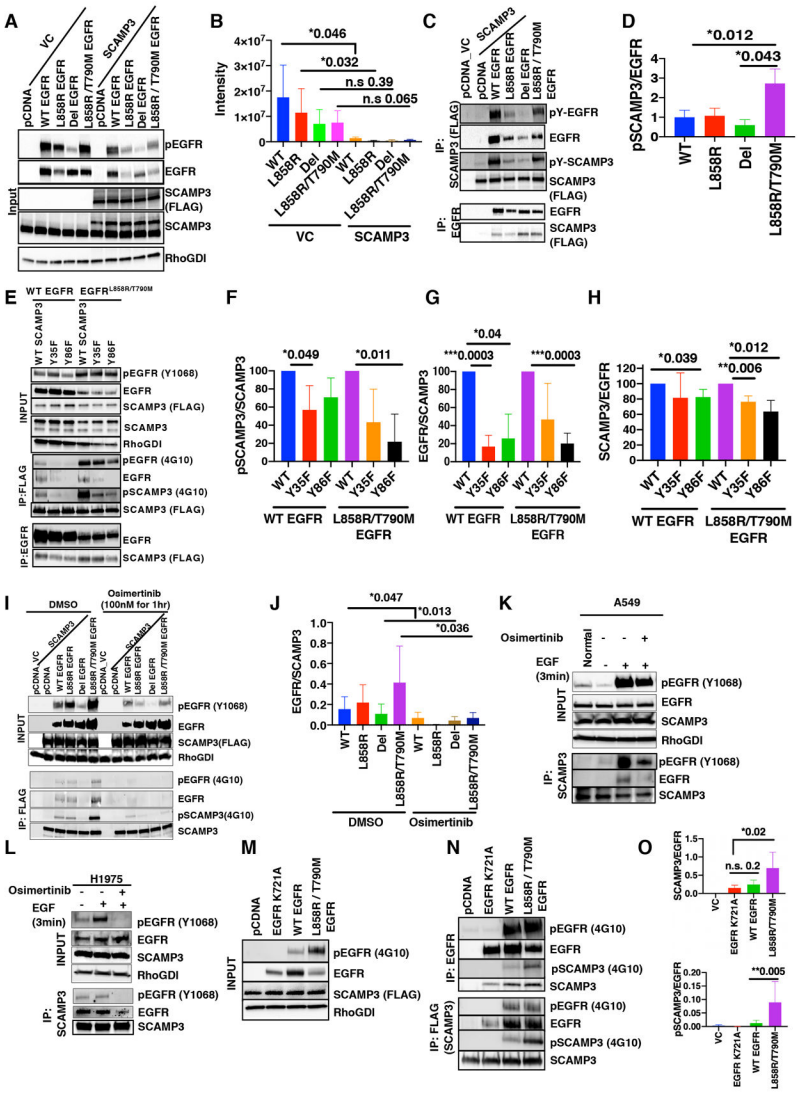

Figure 2. SCAMP3 phosphorylation is EGFR dependent and enhances SCAMP3-EGFR interaction

HEK293T cells stably expressing either vector control or 3xFLAG-SCAMP3 were transiently transfected with constructs expressing pCDNA, WT, L858R, Del or L858R/T790M EGFR. Cell lysates were prepared 72 hours post-transfection. **A,** Lysates were immunoblotted with EGFR, pEGFR, SCAMP3 and RhoGDI (loading control) antibodies to determine input protein levels. This was performed in four biological replicates and the total EGFR intensity quantified by densitometry, **B** and **C**, Lysates were immunoprecipitated with FLAG, then immunoblotted with EGFR, FLAG, pEGFR (4G10), and pSCAMP3 (4G10) antibodies (upper panel) or immunoprecipitated with EGFR and immunoblotted with EGFR and FLAG antibodies (lower panel). Immunoprecipitation was performed in three biological replicates. **D,** pSCAMP3 (4G10) and EGFR immunoblot bands from the immunoprecipitation of SCAMP3 were measured using densitometry and plotted as pSCAMP3 to EGFR ratio. **E**, HEK293T cells were transiently co-transfected with constructs expressing either WT EGFR or L858R/T790M EGFR together with SCAMP3,

SCAMP3 Y35F or SCAMP3 Y85F. Cells were lysed and analyzed by immunoblotting with EGFR, pEGFR(Y1068), FLAG, SCAMP3, and RhoGDI (loading control) antibodies (upper panel). Lysates were immunoprecipitated with FLAG antibodies and immunoblotted with pEGFR (4G10), EGFR, pSCAMP3 (4G10) and FLAG antibodies (middle panel), or immunoprecipitated with EGFR antibody and immunoblotted with EGFR and FLAG antibodies (lower panel). These experiments were performed in three biological replicates. We quantified the bands by densitometry and plotted pSCAMP3 to SCAMP3 ratio, **F**, EGFR to SCAMP3 ratio from SCAMP3 (FLAG) immunoprecipitation experiments, **G**, and SCAMP3 to EGFR ratio from EGFR immunoprecipitation experiments, **H**. In all these plots, the condition of WT SCAMP3 was considered as 100%. **I**, HEK293T cells with stable expression of either vector control or 3xFLAG tagged SCAMP3 were transiently transfected with constructs expressing pCDNA, WT EGFR, L858R EGFR, Del EGFR or L858R/T790M EGFR. Cells were treated with either DMSO or osimertinib (100nM for 1 hour). Cells were lysed and analyzed by immunoblotting with pEGFR (Y1068), EGFR, FLAG and RhoGDI (loading control) antibodies (upper panel). Lysates were immunoprecipitated with FLAG antibodies, then analyzed by immunoblotting with pEGFR (4G10), EGFR, pSCAMP3 (4G10), and SCAMP3 antibodies (lower panel). Three biological replicates were conducted for these experiments. **J**, EGFR to SCAMP3 ratio from SCAMP3 immunoprecipitation was calculated and plotted. **K**, A549 cells were grown in normal medium or serum starved for 18 hours. Serum starved cells were treated with either EGF (100ng/ml for 3 minutes) alone or together with osimertinib (100nM for 1 hour). Lysates were immunoblotted with pEGFR (Y1068), EGFR, SCAMP3, and RhoGDI (loading control) antibodies (top panel). Lysates were immunoprecipitated with SCAMP3 antibody and immunoblotted with EGFR and SCAMP3 (bottom panel). **L**, H1975 cells were either serum starved for 18 hours or serum starved for 18 hours followed by EGF (100ng/ml for 3 minutes) treatment alone or prior osimertinib (100nM) treatment for 1 hour. Cells were lysed and immunoblotted with pEGFR (Y1068), EGFR, SCAMP3 and RHOGDI (loading control) antibodies (upper panel). Lysates were immunoprecipitated with SCAMP3 antibodies, and immunoblotted with pEGFR (Y1068), EGFR and SCAMP3 antibodies (lower panel). **M,** HEK293T cells were transiently co-transfected with constructs expressing either pcDNA, EGFR K721A, WT EGFR or L858R/T790M EGFR along with SCAMP3. Cells were lysed and analyzed by immunoblotting with EGFR, pEGFR (4G10), FLAG-SCAMP3, and RhoGDI (loading control) antibodies. **N**, These lysates were immunoprecipitated with either EGFR or FLAG antibodies and immunoblotted with pEGFR (4G10), EGFR, pSCAMP3 (4G10) and SCAMP3 antibodies. **O**, This experiment was performed in three biological replicates and intensities of SCAMP3, EGFR, pEGFR(4G10) and pSCAMP3(4G10) from the immunoblots were plotted as SCAMP3/EGFR ratio (top panel) and pSCAMP3/EGFR ratio (bottom panel). *P* value was calculated between two groups using a paired *t* test, except in figures **F**, **H** and **O**, where we used an unpaired *t* test; $*P < 0.05$ indicates a significant difference. **G**, data was analyzed for multiple testing using Benjamini, Krieger and Yekutieli method and q value provided. *q<0.05, **q<0.01, ***q<0.005 indicates a significant difference upon multiple testing. In the box plots error bars indicate mean ± S.E.M.

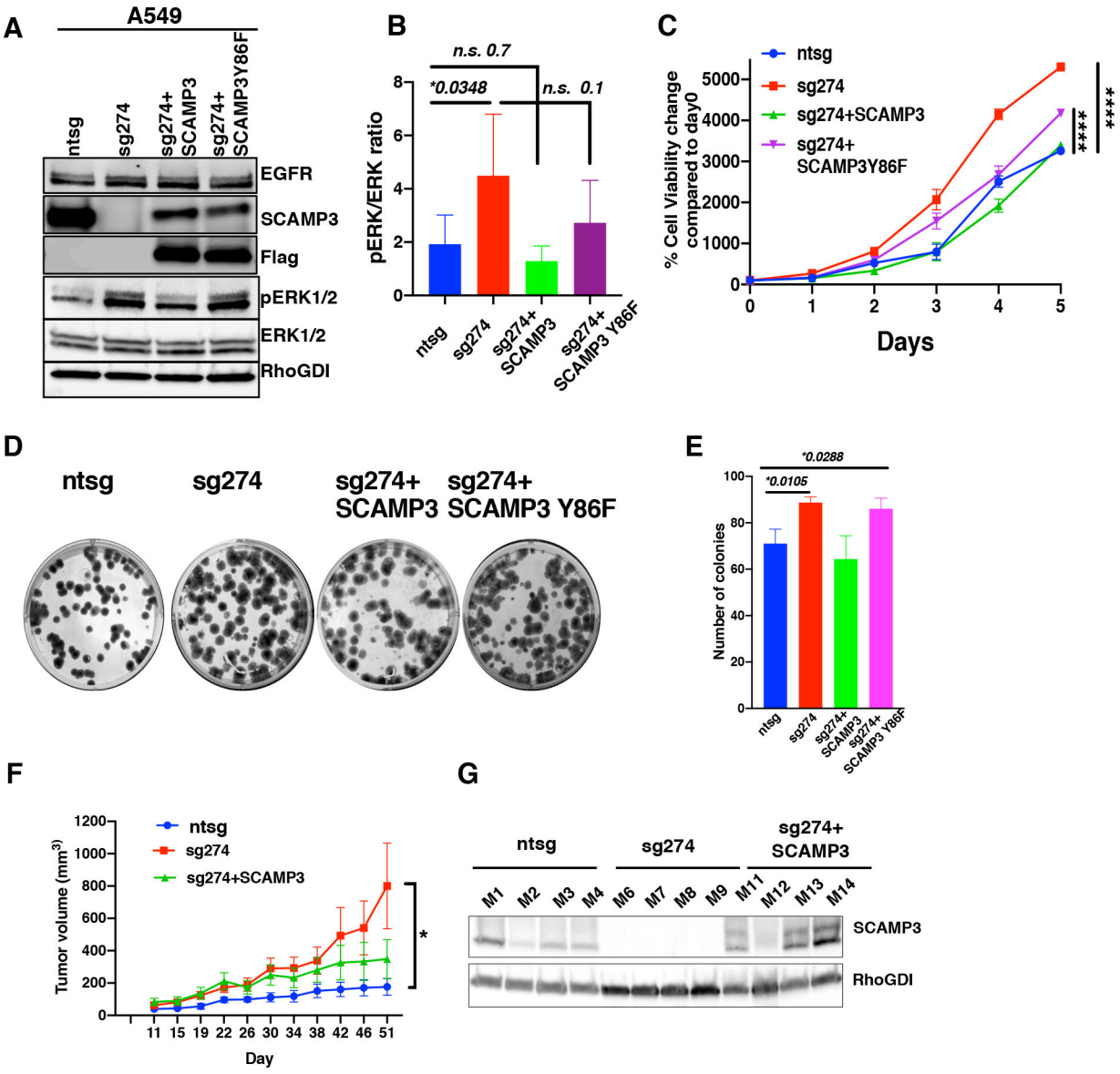

Figure 3. SCAMP3 depletion accelerates tumor growth in human lung adenocarcinoma cells expressing EGFR^{WT}

SCAMP3 was depleted from A549 cells by CRISPR: Non-targeted sgRNA control (ntsg), SCAMP3 depleted (sg274), SCAMP3 rescue (sg274+SCAMP3) and SCAMP3 Y86F rescue cells were generated. **A,** Cells were lysed and immunoblotted with EGFR, SCAMP3, FLAG, total ERK1/2 and phospho-ERK1/2 and RhoGDI (loading control) antibodies. **B**, Total ERK1/2 and phospho-ERK1/2 immunoblots were measured from three biological replicates and plotted as given in the figure. **C**, Cell viability was measured for 5 days (n=4) and significant differences between the groups at 5th day were calculated using unpaired *t* test. **D and E,** Colony formation was assayed and quantitated (n=4). Xenografts were generated using the cells (ntsg, sg274 and sg274+SCAMP3) and **F,** Tumor volume was measured (n=5 in each group). **G,** Xenograft lysates were immunoblotted with SCAMP3 and RhoGDI (loading control) antibodies. *P* value was calculated between two groups using unpaired *t*

test, except for figure B, where we used paired *t* test; **P* < 0.05, ***P* <0.01, ****P* <0.005, indicates a significant difference between groups. Figure **C** and **E** were further analyzed for multiple testing using Benjamini, Krieger and Yekutieli method and q value provided. *q<0.05, ****q<0.001 indicates a significant difference upon multiple testing. Error bars# s.e.m and n indicates biological replicates.

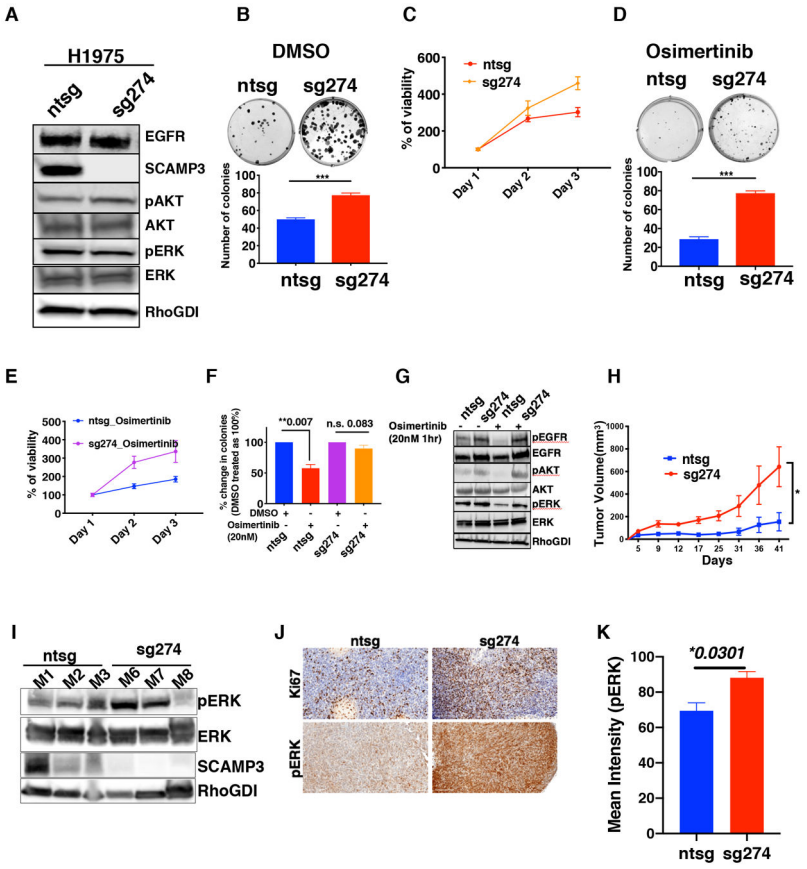

Figure 4. SCAMP3 depletion accelerates tumor growth in human lung adenocarcinoma cells expressing EGFR$^{L858R/T790M}$ and may decrease sensitivity to EGFR TKI

A, SCAMP3 was depleted in H1975 cells by CRISPR: H1975 with SCAMP3 knocked out (sg274), and control non-targeted sgRNA control (ntsg) were immunoblotted with the indicated antibodies (n=3). **B** and **C,** Colony formation and proliferation of cells treated with DMSO was assayed and quantitated (n=3). **D** and **E,** H1975 cells with non-targeted sgRNA and SCAMP3 knockout cells were analyzed for colony formation and cell proliferation with 20nM osimertinib (n=3 biological replicates). **F,** quantitated and plotted percent change of colony formation upon treatment with osimertinib. DMSO treated ntsg and sg274 cell viability was considered as 100% and the observed percent of decrease was calculated by comparing osimertinib treatment to DMSO. **G,** H1975 cells with control and SCAMP3 knockout cells were treated with osimertinib (20nM) for 1hr and lysed the cells, immunoblotted with the pEGFR, total EGFR, pAKT(S473), total AKT, pERK and total ERK. Experiment was performed as biological replicates (n=2). **H**, SCAMP3 depleted and ntsg control H1975 cells were injected into athymic nu/nu mice to generate xenografts and tumor volume (n=6 for each group) was plotted**. I,** Xenograft tumor lysates were immunoblotted with the indicated antibodies. **J**, Immunohistochemistry of tumor sections derived from the xenografts shows Ki67 and pERK staining. **K**, pERK staining from the immunohistochemistry of xenograft tumor sections were quantified and plotted (n=3 in each group). *P* value was calculated using Welch's *t* test between two groups as indicated in the

figure and shown in each panel; *$P < 0.05$, **$P < 0.01$, ***$P < 0.005$, indicates a significant difference, error bars indicate mean ± S.E.M.

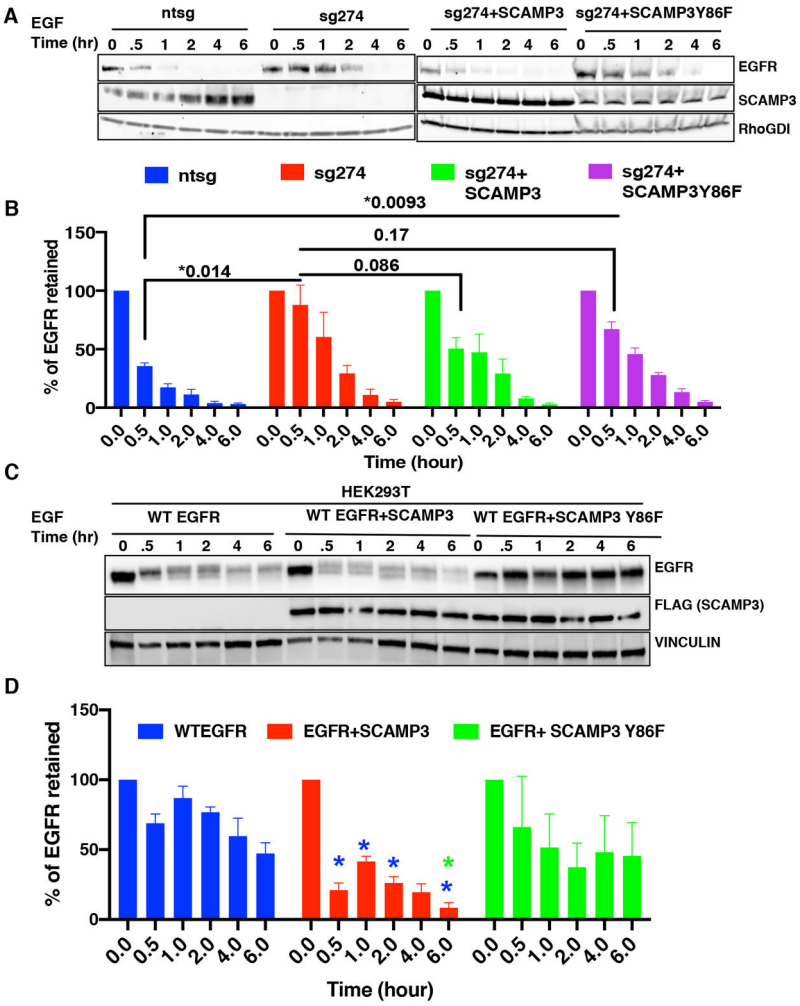

Figure 5. SCAMP3 enhances EGFR degradation upon EGF stimulation

A, A549 non-targeted sgRNA control (ntsg), SCAMP3 depleted (sg274), and SCAMP3 rescue (sg274+SCAMP3) cells were serum starved overnight, treated with cycloheximide for 1 hour, then EGF stimulated (100ng/ml). Cell lysates were prepared at indicated times points and immunoblotted with EGFR, SCAMP3 and RhoGDI antibodies. **B,** The experiment was repeated three times and EGFR intensity at various timepoints was measured and plotted on the graph. **C**, HEK293T cells stably expressing WT EGFR alone or together with SCAMP3 were serum starved overnight and treated with cycloheximide for 1 hour prior to EGF (100ng/ml) stimulation. Lysates were prepared at indicated time points, and immunoblotted with EGFR, FLAG (SCAMP3) and vinculin antibodies. **D**, The experiment was repeated thrice, and measured EGFR intensities and plotted the graph indicating residual EGFR in various timepoints. Calculated significant differences (*P* value) between the groups using paired two tailed *t* tests. **P* <0.05, indicates a significant difference, error bars indicate mean ± S.E.M.

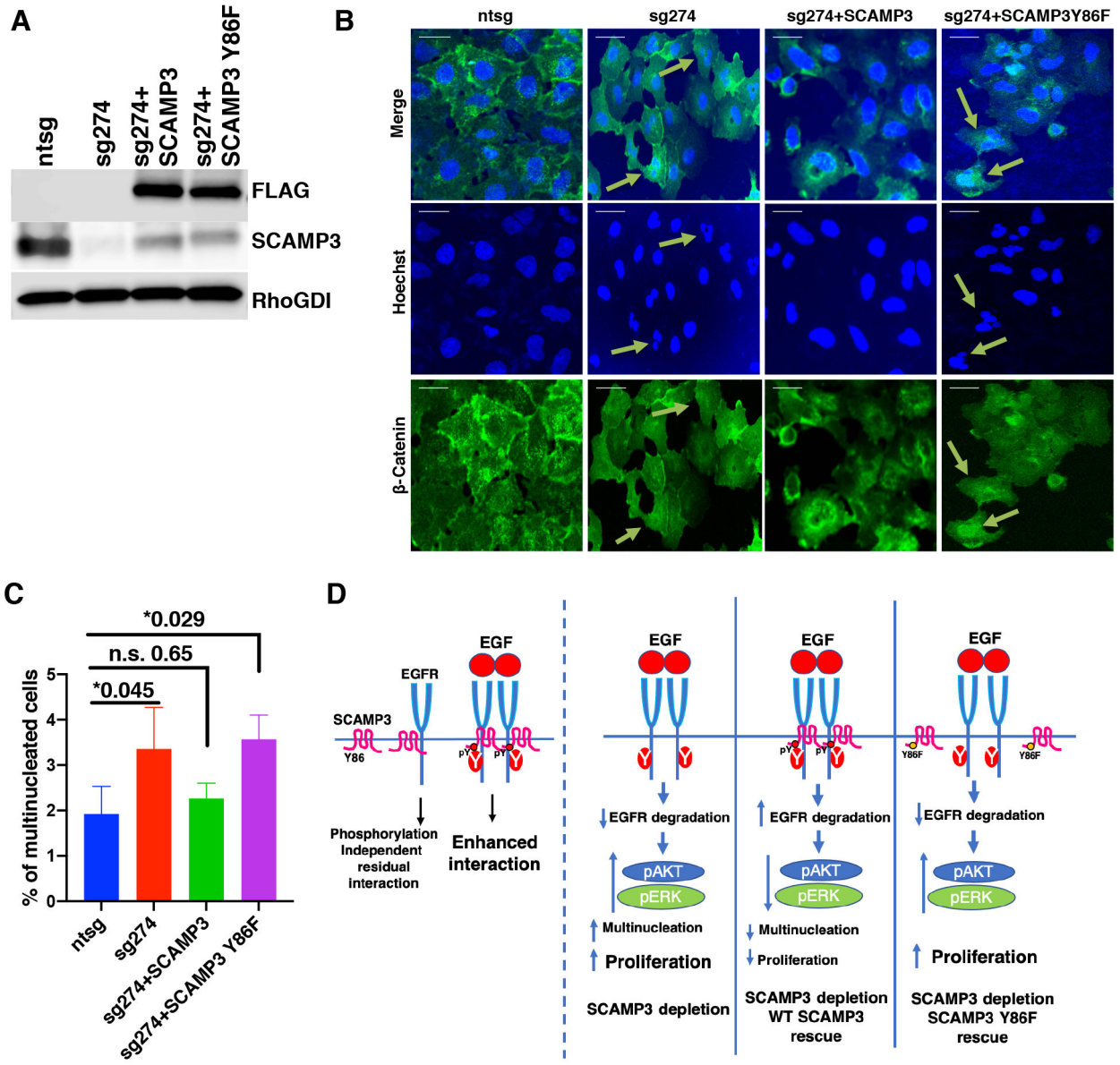

Figure 6. SCAMP3 depletion alters nuclear number and morphology in lung adenocarcinoma

SCAMP3 was depleted from A549 cells by CRISPR: Non-targeted sgRNA control (ntsg), SCAMP3 depleted (sg274), SCAMP3 rescue (sg274+SCAMP3) and SCAMP3 Y86F rescue cells were generated. **A,** Cells were lysed and immunoblotted with FLAG, SCAMP3, and RhoGDI (loading control) antibodies. **B,** Representative confocal micrographs of control A549 cells, SCAMP3 depleted and SCAMP3 depleted and rescued with either SCAMP3 or SCAMP3 Y86F. Cells were stained with β-Catenin and Hoechst 33342 without permeabilizing, and confocal images were obtained at 20X. Scale bar# 50μm. **C,** Bar-graphs showing the percentage of multinucleated cells in ntsg control cells (n=1576), SCAMP3 depleted cells (n=1132), SCAMP3 depleted cells rescued using SCAMP3 (n=1283), and SCAMP3 Y86F (n=1041). Arrows point to representative multinucleated nuclei. **D**, Cartoon summarizing the findings in this study. Left panel shows the membrane bound

SCAMP3 and EGFR proteins. EGF ligand stimulation results in EGFR dimerization and phosphorylation that in turn results in phosphorylation of SCAMP3 and enhanced EGFR-SCAMP3 interaction. There is a minor fraction of SCAMP3 that interacts with EGFR even in the absence of EGFR and SCAMP3 phosphorylation. Right panel shows the findings in the context of SCAMP3 depletion and SCAMP3 depletion rescued with either wild type SCAMP3 or SCAMP3 Y86F. SCAMP3 depletion results in decreased degradation of EGFR, increased downstream signaling, multinucleation, and increased proliferation. Degradation, multinucleation and proliferation phenotypes are rescued by wild type SAMP3, but not SCAMP3 Y86F.